

---

# Anatomy of the Modality Gap: Dissecting the Internal States of End-to-End Speech LLMs

---

Ming-Hao Hsu<sup>1</sup> Xueyao Zhang<sup>1</sup> Xiaohai Tian<sup>2</sup> Jun Zhang<sup>2</sup> Zhizheng Wu<sup>1</sup>

## Abstract

Recent advancements in Large Speech-Language Models have significantly bridged the gap between acoustic signals and linguistic understanding. However, a persistent performance disparity remains in speech-based input tasks compared to direct text inference. In this paper, we investigate the *dynamic* roots of this modality gap beyond static geometric alignment, analyzing how speech and text representations evolve layer-by-layer. We evaluate four open-weight end-to-end models on SpeechMMLU and VoiceBench BBH. Using cross-layer CKA analysis with speech-text token alignment, we find that speech representations exhibit a broad cross-layer alignment band, attributable to the redundant nature of speech where semantic content spans multiple frames. We show that these alignment patterns are structurally stable across different analysis configurations. Crucially, simple statistical calibration is insufficient and can be detrimental when applied at the input layer, indicating that the modality gap is not a mere distribution shift. Overall, our results suggest that the bottleneck lies in condensing redundant speech into stable late-layer decisions, motivating future solutions that operate at the token or temporal granularity instead of feature-level matching.

## 1. Introduction

Recent advancements in Large Speech-Language Models (LSLMs) have significantly bridged the gap between acoustic signals and linguistic understanding, enabling end-to-end models to perform impressive conversational tasks (Chu et al., 2023; Zhang et al., 2023; Goel et al., 2025). Ideally, an LSLM should function as a unified cognitive engine, where speech inputs activate reasoning capabilities com-

parable to their text counterparts. However, a persistent performance disparity remains, stemming from representational differences between modalities, which is commonly termed the Modality Gap (Chen et al., 2024; Team et al., 2025; Mousavi et al., 2025). Even when an LSLM accurately transcribes speech, it consistently underperforms on complex reasoning and knowledge benchmarks compared to direct text inputs (Wang et al., 2026). This suggests that recognition does not imply understanding, and that speech inputs fail to fully leverage the reasoning and knowledge capabilities exhibited by text.

To address this gap, the prevailing research paradigm has viewed the problem through a geometric lens (Park et al., 2024). Most existing approaches operate on the assumption that the modality gap is essentially a distribution shift in the representation space (Wang et al., 2026; Mousavi et al., 2025). Consequently, methodologies have focused on minimizing the Euclidean distance or maximizing the cosine similarity between speech and text embeddings (Xiang et al., 2025). The underlying hypothesis is straightforward: if we can geometrically align the speech representation to overlap with the text manifold, the downstream LLM should process both modalities identically. Under this view, the solution lies in better projectors, contrastive loss functions, or length normalization techniques.

While geometric alignment has driven significant progress, it does not fully account for the nuanced behaviors observed in high-order reasoning tasks (You, 2025; Wang et al., 2026). Our evidence suggests that geometric alignment is a necessary but insufficient condition for functional equivalence: **speech representations can become text-like in mid layers, yet still fail to stably form the correct late-layer decision.** Through diagnostic probing (Alain & Bengio, 2017), we find that simple statistical calibration via mean and variance matching does not recover downstream performance, and enforcing alignment at the input layer can even be detrimental. Together, these results motivate shifting the analysis from static geometry to how representations evolve layer-by-layer (Geva et al., 2021) and how semantic information is distributed across tokens.

Building on recent findings in LLM computational stages (Lad et al., 2024), we propose a new framework

<sup>1</sup>School of Data Science, The Chinese University of Hong Kong, Shenzhen <sup>2</sup>ByteDance. Correspondence to: Zhizheng Wu <wuzhizheng@cuhk.edu.cn>.

that shifts the focus from static geometry to inference dynamics. Using this lens, we identify the root cause of the modality gap as a structural mismatch in semantic information granularity, specifically, the contrast between dense text tokens and redundant speech frames. Text tokens are information-dense and exhibit a late-layer *residual sharpening* phase that supports precise lexical selection, whereas speech tokens are redundant and distributed across frames, thereby hindering this critical sharpening process. Our analysis shows that speech representations align closely with text in mid layers, yet often fail to stably isolate the correct lexical choice in late layers. We attribute this to a mechanism we term **Information Dilution**: stemming from the inherent redundancy of speech, semantic units are spread across multiple frames, leaving the per-token signal too weak to drive a reliable last-mile collapse. The result is a failure mode where representations remain semantically broad, lacking the discriminative sharpness to isolate the correct lexical answer.

We provide a comprehensive anatomy of this mechanism across four open-weight LSLMs. To ensure our diagnostics target the true reasoning gap rather than basic recognition failures, we prioritize models with established S2T capabilities. We uncover three distinct phases of speech input processing in LSLMs:

1. **Phase I: Structural Transformation:** We show that speech features initially reside in a manifold distinct from text, necessitating a transformation phase before alignment can occur. This explains why previous attempts at input-level alignment inherently fail.
2. **Phase II: Semantic Smearing:** We identify a broad cross-layer alignment band across tasks, confirming that speech semantics are smeared due to redundancy rather than mapping one-to-one with text tokens.
3. **Phase III: Decision Instability:** Finally, we demonstrate that even after mid-layer alignment, speech representations fail to stably isolate the correct lexical choice, indicating a failure in the final sharpening process.

In summary, we show that the modality gap stems from the inherent redundancy of speech, which prevents stable decision-making. Our findings suggest that future solutions must go beyond simple feature matching and focus on condensing multiple speech frames into sharper, information-dense units.

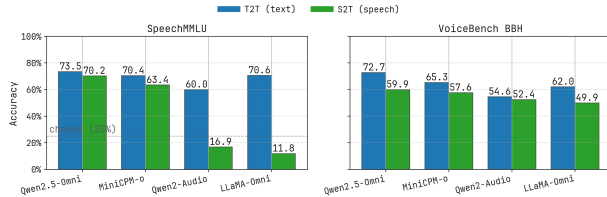


Figure 1. T2T and S2T accuracy comparison across four models. The modality gap, measured as the accuracy drop from text input to speech input, is consistent across all models and both benchmarks.

## 2. Related Work

### 2.1. Large Speech-Language Models and the Reasoning Gap

The integration of speech processing with Large Language Models (LLMs) has evolved from cascade systems (ASR followed by LLM) to end-to-end architectures (Zhang et al., 2023; Chu et al., 2023; Fang et al., 2025a). Recent surveys (Yang et al., 2025; Cui et al., 2025) categorize these models into adapter-based approaches, which map speech features into the LLM’s input space (Chu et al., 2024; Yao et al., 2024), and fully end-to-end models that tokenize speech directly (Goel et al., 2025). While these models achieve impressive performance on speech recognition and translation, a persistent *intelligence degradation* has been observed when they perform complex reasoning tasks with speech inputs compared to text (Chen et al., 2024; Fang et al., 2025b). Wang et al. (2026) and Chen et al. (2024) highlight that this performance drop, often termed the *Modality Gap*, remains significant even when the underlying LLM is frozen and highly capable. Our work moves beyond benchmarking this gap to diagnosing its internal mechanistic causes.

### 2.2. Geometric Alignment and Modality Heterogeneity

The prevailing perspective attributes the modality gap to geometric heterogeneity between embedding spaces. Liang et al. (2022) identified the *Cone Effect* in vision-language models, where modalities occupy disjoint regions. In the speech domain, Mousavi et al. (2025) and Xiang et al. (2025) quantified the misalignment between speech and text representations, proposing that maximizing cosine similarity or minimizing Euclidean distance would resolve the issue. However, recent findings suggest that geometric alignment is a necessary but insufficient condition for reasoning. You (2025) argued that cosine similarity can be misleading in high-dimensional spaces. Critically, existing alignment techniques primarily focus on the input or shallow layers. Our analysis reveals that even when representations appear aligned in intermediate layers, they may still fail to drive the correct decision dynamics in deeper layers, suggesting the need for a perspective shift from static geometry to dynamic

inference trajectories.

### 2.3. Mechanistic Interpretability of Multimodal Models

Understanding the layer-wise information processing of LLMs has been advanced by techniques like the Logit Lens (nostalgebraist, 2020) and Tuned Lens (Belrose et al., 2023), which decode hidden states into vocabulary distributions. Lad et al. (2024) utilized these tools to decompose LLM inference into functional stages, identifying a critical *residual sharpening* phase in the final layers. In the multimodal domain, mechanistic interpretability is nascent. Glazer et al. (2025) and Ma et al. (2025) applied Logit Lens to analyze ASR and speech emotion recognition systems, revealing how acoustic features evolve into semantic ones. However, these studies focused on recognition and classification tasks. To the best of our knowledge, our work is the first to apply these interpretability frameworks to *reasoning* tasks in LSLMs, specifically isolating where and why the reasoning process diverges between speech and text modalities.

### 2.4. Information Density and Redundancy in Speech

A fundamental distinction between speech and text lies in information density. Speech is inherently continuous and redundant, whereas text is discrete and information-dense. Zuo et al. (2025) noted the mismatch between speech token rates (25-50 Hz) and semantic word rates (2-5 Hz). Dorszewski et al. (2025) demonstrated that the transformer stack in speech models exhibits significant redundancy, with many layers contributing marginally to the final representation. While previous works viewed this redundancy primarily as an efficiency bottleneck (Liu et al., 2025), we argue that it fundamentally hinders the reasoning process. Our analysis suggests that the diffuse nature of speech information prevents the formation of the sharp, low-entropy states required for the LLM’s final decision-making phase, acting as a precision bottleneck rather than just a computational one.

## 3. Methodology

In this section, we establish the analytical framework, define the modality gap formally, and describe our measurement protocol.

### 3.1. Problem Formulation

We consider end-to-end Large Speech-Language Models (LSLMs) that accept either text or speech as input and generate text outputs. We denote these two evaluation modes as T2T (text-to-text) and S2T (speech-to-text), respectively.

Let  $\mathcal{M}$  be an LSLM and  $x$  be a semantic query. Let  $x_{\text{text}}$  denote the textual form such as a transcription, and  $x_{\text{speech}}$

denote an acoustic realization conveying the same content. Let  $\mathcal{P}(\cdot)$  be a task-dependent performance metric computed against ground-truth labels, such as accuracy. We define the *speech-text modality gap* on an instance as

$$\Delta(x) = \mathcal{P}(\mathcal{M}(x_{\text{text}})) - \mathcal{P}(\mathcal{M}(x_{\text{speech}})),$$

and its dataset-level counterpart as  $\Delta_{\mathcal{D}} = \mathbb{E}_{x \sim \mathcal{D}}[\Delta(x)]$ .

A positive gap ( $\Delta_{\mathcal{D}} > 0$ ) indicates that, under matched semantics, performance degrades when switching the input modality from text to speech. Notably,  $\Delta_{\mathcal{D}}$  can remain positive even when transcription quality is high, suggesting that the bottleneck lies beyond perception and into semantic inference and decision formation.

## 3.2. Models and Datasets

### 3.2.1. MODELS

We study four open-weight end-to-end speech-language models: **Qwen2.5-Omni-7B** (Xu et al., 2025), **MiniCPM-o 2.6** (Yao et al., 2024), **Qwen2-Audio-7B-Instruct** (Chu et al., 2024), and **LLaMA-Omni** (Fang et al., 2025a). All models accept either audio for S2T or text for T2T as the user input modality and generate text answers. Our analyses are designed to be model-agnostic: we extract internal hidden states under matched prompts and compare S2T versus T2T dynamics using the same alignment and diagnostic pipeline.

To contextualize the behavioral modality gap for each model, we report baseline accuracies for SpeechMMLU and VoiceBench BBH in Figure 1. Unless otherwise stated, the deeper diagnostic suite including margin analysis, Layer-Norm controls, and calibration interventions is run on models with non-trivial S2T knowledge performance, namely Qwen2.5-Omni-7B and MiniCPM-o. We report additional models that fall into a near-chance S2T SpeechMMLU regime, specifically Qwen2-Audio and LLaMA-Omni, in Section E for completeness and failure-mode context.

### 3.2.2. DATASETS

**SpeechMMLU (Massive Multitask Language Understanding - Speech)**. SpeechMMLU (Hendrycks et al., 2021; Team et al., 2025) is adapted from the standard MMLU benchmark, which covers 57 subjects across STEM, the humanities, and social sciences. We synthesize each question and its answer options into audio waveforms using a high-quality text-to-speech system, turning MMLU into a knowledge benchmark under speech input. This setting evaluates whether domain knowledge and terminology remain usable when the input modality is switched from text to speech.

**VoiceBench BBH (BIG-Bench Hard - Speech)**. VoiceBench BBH is adapted from BIG-Bench Hard

(BBH) (Suzgun et al., 2023), a subset of 23 challenging tasks from the BIG-Bench suite where traditional language models often struggle. These tasks focus on multi-step reasoning, logical deduction, and algorithmic thinking. In our experiments, we use the VoiceBench-bbh subset with four tasks, namely `hyperbaton`, `navigate`, `sports_understanding`, and `web_of_lies`. Similar to SpeechMMLU, complex logical puzzles are converted into audio clips. By presenting problems as transient audio, VoiceBench BBH serves as a stress test of working-memory and reasoning stability under speech input, requiring the model to operate on acoustic sequences rather than static text.

### 3.3. Alignment Methods and Metrics

To rigorously evaluate the representational convergence between the speech and text modalities within the model, we employ a set of geometric and structural similarity metrics. Since speech and text sequences naturally possess different lengths and granularities, we first establish a monotonic alignment between them. Subsequently, we apply three distinct metrics to quantify the cross-modal alignment: Cross-Modal Centered Kernel Alignment (CKA), Layer-wise Token Norm, and Standardized Euclidean Distance.

#### 3.3.1. SPEECH-TEXT TOKEN ALIGNMENT

A primary challenge in comparing speech and text representations is the length mismatch. Speech sequences  $S$  typically contain significantly more frames than their corresponding text tokens  $T$ . To address this, we utilize Dynamic Time Warping (DTW) to find an optimal monotonic alignment path. Intuitively, this aligns the temporal progression of speech frames to match the discrete steps of text tokens, which is a prerequisite for metrics like CKA that require paired samples. For all analyses, we extract hidden states from the last user turn (the question itself) to focus on the reasoning process.

Let  $H^S \in \mathbb{R}^{T_s \times D}$  and  $H^T \in \mathbb{R}^{T_t \times D}$  denote the hidden state sequences for speech and text, respectively, derived from a selected base layer of the model. We first compute a pairwise similarity matrix  $M \in \mathbb{R}^{T_s \times T_t}$  based on cosine similarity:

$$M_{i,j} = \frac{H_i^S \cdot (H_j^T)^\top}{\|H_i^S\|_2 \|H_j^T\|_2}$$

We then efficiently find the alignment path that maximizes the cumulative similarity. Let  $D_{i,j}$  be the cumulative score at grid position  $(i, j)$ . The recurrence relation is defined as:

$$D_{i,j} = M_{i,j} + \max(D_{i-1,j}, D_{i,j-1}, D_{i-1,j-1})$$

Backtracking from  $(T_s, T_t)$  yields the optimal path  $P = \{(i_k, j_k)\}_{k=1}^K$ . This path is used to warp the sequences into

aligned pairs, allowing for direct token-wise comparison in subsequent metric calculations.

#### 3.3.2. SIMILARITY METRICS

**Cross-Modal Centered Kernel Alignment (CKA).** To assess the structural similarity between speech and text representations independent of invertible linear transformations, we employ Linear CKA with double-centering. Given aligned speech feature matrix  $X \in \mathbb{R}^{N \times D}$  and text feature matrix  $Y \in \mathbb{R}^{N \times D}$ , we first construct the linear Gram matrices  $K = XX^\top$  and  $L = YY^\top$ .

We apply the centering matrix  $H = I_N - \frac{1}{N}\mathbf{1}\mathbf{1}^\top$  to obtain centered Gram matrices  $K' = HKH$  and  $L' = HLY$ . The CKA score is computed as the normalized Hilbert-Schmidt Independence Criterion (HSIC):

$$\text{CKA}(X, Y) = \frac{\langle K', L' \rangle_F}{\|K'\|_F \|L'\|_F}$$

where  $\langle \cdot, \cdot \rangle_F$  denotes the Frobenius inner product. A CKA score closer to 1.0 indicates that the speech and text modalities share a highly similar representational geometry.

**Standardized L2 Distance.** While CKA measures structural correlation, it is invariant to scaling and shifting. To measure the direct geometric proximity of the aligned embeddings, we compute the Standardized L2 Distance. The standard Euclidean distance can be dominated by the varying scales of different layers. Therefore, we standardize the hidden states along the feature dimension before calculating the distance.

For an aligned pair of vectors  $x$  (speech) and  $y$  (text) at a specific layer, we define the standardization function  $\phi(\cdot)$  such that  $\phi(v) = \frac{v - \mu_v}{\sigma_v + \epsilon}$ . The metric is defined as:

$$\mathcal{D}_{\text{std}}(X, Y) = \frac{1}{N} \sum_{k=1}^N \|\phi(x_k) - \phi(y_k)\|_2$$

**Layer-wise Mean Token Norm.** To investigate the amplitude differences between modalities, we compute the mean L2 norm of the representation vectors for each layer. For a given modality with representations  $Z \in \mathbb{R}^{N \times D}$ , the layer-wise norm is:

$$\text{Norm}(Z) = \frac{1}{N} \sum_{k=1}^N \|z_k\|_2$$

This metric helps identify if the model relies on significantly different activation magnitudes to encode speech versus text information.

## 4. Empirical Analysis

We now validate our analytical framework through layer-wise diagnostics on SpeechMMLU and VoiceBench BBH

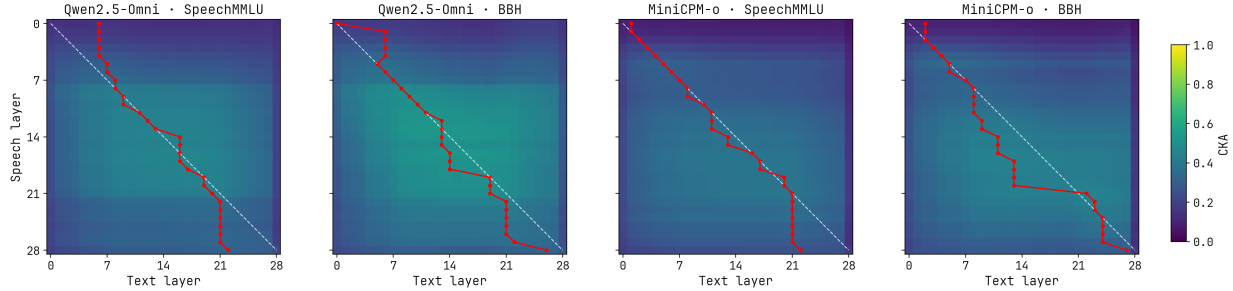


Figure 2. **Cross-modal cross-layer CKA heatmaps.** Each heatmap compares S2T layers on the y-axis against T2T layers on the x-axis. The early dark zone indicates Phase I heterogeneous projection, the broad diagonal band reflects Phase II semantic smearing, and late-layer stagnation reveals Phase III decision instability.

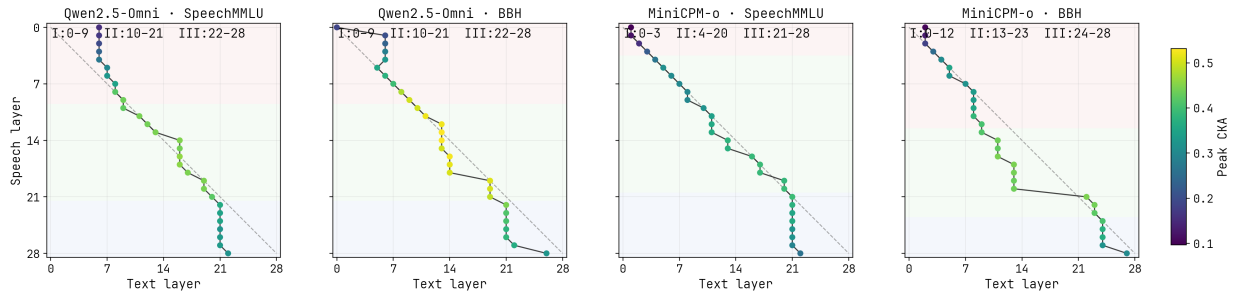


Figure 3. **Phase boundary visualization from CKA summaries.** Black lines show best-match paths; point colors indicate row-wise peak alignment strength. Background shading marks the three processing phases. The late-layer plateau reveals where speech representations stall before reaching the text head.

across four end-to-end speech LLMs. Figure 1 establishes the behavioral modality gap, showing that all models have substantial S2T performance drops. For instance, Qwen2.5-Omni exhibits a 6.7% drop on SpeechMMLU and 3.9% on BBH, while MiniCPM-o shows more pronounced gaps of 13.8% on SpeechMMLU and 10.2% on BBH. Unless otherwise stated, we use Qwen2.5-Omni as the primary case study for internal diagnostics and report additional results in the Appendix.

To analyze the modality gap, we structure our analysis into three phases, namely Structural Transformation, Semantic Smearing, and Decision Instability. **Phase I: Structural Transformation.** We investigate whether speech adapter outputs initially reside in a manifold distinct from text embeddings, requiring early Transformer layers to perform a non-linear projection before alignment becomes possible. **Phase II: Semantic Smearing.** We examine if speech’s inherent redundancy, where a single semantic unit spans multiple frames, manifests as distributed cross-layer alignment rather than sharp 1:1 token correspondence with text. **Phase III: Decision Instability.** We analyze whether speech representations, even after achieving mid-layer geometric alignment, fail to complete the final decision-making process due to weak per-token signals. This framework guides our empirical analysis in the following subsections, where

we test each phase through complementary diagnostics. We report detailed implementation choices in Section I.1.

**Quantifying Phase Boundaries.** To make the three phases numerically explicit, we summarize each CKA heatmap by two metrics, the row-wise peak alignment and the best-match text layer for each speech layer. The Phase I to II boundary is identified as the change-point where peak alignment begins to rise, detected via a two-segment piecewise linear fit. Phase III begins when the best-match path plateaus for at least 3 consecutive layers after 60% depth. Figure 3 visualizes these boundaries and reports the resulting layer ranges for both models. We verify the robustness of these alignment paths to DTW hyperparameters in Section A.1.

In the early layers, speech representations have low similarity to *any* text layer, corresponding to the early dark zone shown in Figure 2. This indicates that the speech adapter output is not directly in the same feature geometry as text embeddings, and that early Transformer layers act as a *non-linear projector* that re-parameterizes speech features before they become text-like. As a result, heterogeneous projection is a *structural transformation* rather than a simple geometric alignment.

As shown in Figure 3, Phase II exhibits a clear lift in peak alignment over Phase I, with average peak alignment 1.5–2.3

Method	BBH Accuracy	$\Delta$ vs Baseline
None (baseline)	<b>62.3%</b>	—
Input (layer 0)	46.8%	-15.5%
Output (last layer)	61.2%	-1.1%

Table 1. **Effect of mean and std calibration on BBH.** Calibrating at the input breaks early-layer projection, while calibrating at the output does not recover performance. These results rule out a simple distribution-shift explanation.

times higher than Phase I across both models and benchmarks.

#### 4.1. Phase I: Structural Transformation

Prior work implicitly assumes that speech adapter outputs should directly align with text embeddings. However, our cross-layer CKA analysis in Figure 2 reveals an early dark zone in the shallow layers for both models on both tasks. This indicates that speech features initially reside in a manifold structurally distinct from text. Consequently, early Transformer layers must first perform a non-linear projection before alignment becomes possible.

**Characterizing the nature of structural mismatch.** The observed mismatch could arise from either simple distributional differences such as different mean and variance, or fundamental geometric incompatibility requiring non-linear transformation. To distinguish these two scenarios, we test whether forcing statistical alignment at the adapter output, i.e., Layer 0, can eliminate the gap. We calibrate speech representations to match the mean and standard deviation of text embeddings. Table 1 shows that this intervention causes catastrophic performance collapse of  $-15.5\%$  on BBH. This demonstrates that the structural mismatch is not merely distributional but geometrically fundamental. Early Transformer layers must perform non-linear re-parameterization rather than simple rescaling.

#### 4.2. Phase II: Semantic Smearing

As shown in Figure 2, similarity concentrates into a broad band in the middle layers rather than a sharp diagonal correspondence. This broad alignment pattern arises from the inherent information density difference between modalities. While text tokens are semantically dense, speech units are highly redundant and distributed across multiple frames. Consequently, the transition from acoustic to semantic representations occurs gradually across the speech layers, resulting in a broad correspondence band rather than a precise layer-to-layer mapping (Dorszewski et al., 2025). To quantify this smearing, we measure how many text layers each speech layer aligns with near its peak CKA value. On SpeechMMLU, each speech layer aligns with approxi-

Metric (decision token)	T2T	S2T	$\Delta$
Entropy <sub>norm</sub>	0.361	0.657	+0.289
$p_{\max}$	0.638	0.105	-0.477
Top-10 mass	0.933	0.483	-0.456
Cov <sub>0.90</sub> (fraction)	0.083	0.123	+0.039
Cov <sub>0.90</sub> (count)	8	101	+93

Table 2. **Decision-token attention dispersion.** For each sample we select the attention head that maximizes the entropy gap between S2T and T2T, then select the layer where this gap is largest. We report the median metrics across SpeechMMLU samples. Cov<sub>0.90</sub> is the minimal fraction or count of input tokens whose cumulative attention reaches 90%.

mately 6 text layers on average for both Qwen2.5-Omni and MiniCPM-o, indicating a broad alignment band rather than tight diagonal correspondence.

**Micro-Dynamics of Dilution.** To check if this smearing is a functional bottleneck rather than a geometric artifact, we inspect the attention mechanism at the token level. We trace the attention distribution of the final decision token back to the input sequence. As visualized in Figure 4, there is a clear contrast in attention weight distribution. Since different attention heads serve different functions, we analyze the distribution of per-layer head entropies and report both tail statistics and single-head trajectories. As shown in Table 2, across a random subset of SpeechMMLU questions, the decision-token attention in speech remains systematically more diffuse than text. Compared to text, speech shows higher normalized entropy (0.66 vs 0.36), indicating that attention is spread more uniformly across tokens rather than concentrating on a few. The peak attention mass drops from 0.64 to 0.11, meaning the single most-attended token receives far less focus. Similarly, the top-10 token mass drops from 0.93 to 0.48, indicating that even the most relevant tokens collectively fail to capture the majority of attention. Most directly, capturing 90% of decision attention requires only 8 text tokens but 101 speech tokens, indicating that redundancy prevents the attention mechanism from isolating a sharp semantic signal. This directly links the macro-level smearing observed in CKA to the micro-level failure to form a stable decision. Because individual speech tokens carry weak signals, the model cannot gather enough information in a single layer. Instead, it spreads the information-gathering process across many layers. This explains why Phase II shows a broad alignment band. The model needs multiple layers to collect the distributed speech signal, while text can be processed more efficiently.

**Validating Redundancy as a Causal Factor.** To establish a causal link between redundancy and performance degradation, we perform a controlled intervention on Qwen2.5-

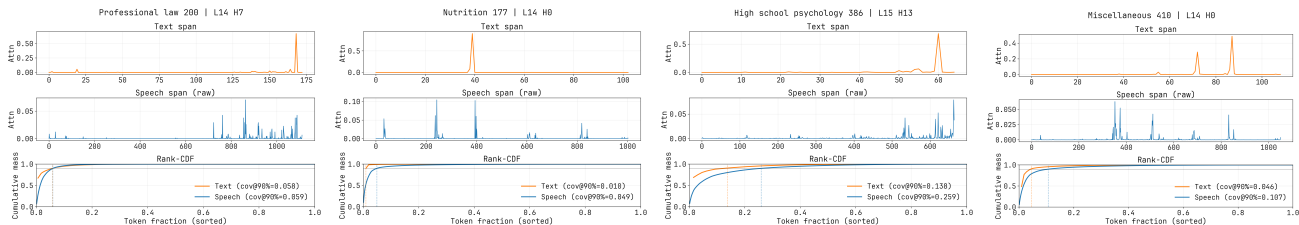


Figure 4. Micro-evidence of Information Dilution (four representative cases). Each panel traces the decision-token attention back to the input span without any resampling. Across diverse questions, text attention consistently sharpens onto a small set of tokens, whereas speech attention spreads mass across many acoustic tokens. The rank-CDF in each panel quantifies this dispersion without requiring sequence-length alignment.

Redundancy	SpeechMMLU		VoiceBench BBH	
	Acc.	Entropy	Acc.	Entropy
$r$				
1	73.9%	0.038	62.4%	0.088
2	67.4%	0.056	56.2%	0.107
4	57.3%	0.069	55.4%	0.106
8	51.2%	0.074	53.5%	0.097

Table 3. Effect of injecting token redundancy into text input. We synthetically increase word-level redundancy in the T2T input by repeating each word  $r$  times and evaluate Qwen2.5-Omni on both benchmarks. Higher redundancy consistently degrades accuracy and increases decision-step entropy, supporting the hypothesis that redundant tokens impede late-layer stabilization.

Omni. We inject artificial redundancy into the T2T input by repeating each word in the question stem 1, 2, 4, or 8 times while keeping the answer options unchanged. Table 3 shows that increasing redundancy alone degrades accuracy on both benchmarks while increasing decision-step entropy. This supports the hypothesis that redundant tokens dilute per-token decision evidence and hinder late-layer sharpening.

**Layer-wise transformations remain coordinated.** Crucially, the broad band is not random drift. As shown in Figure 5, the layer-wise update vectors exhibit high cosine similarity between speech and text, indicating that the transformations applied at each layer are synchronized even when the cross-layer geometry exhibits a broad band. This supports the interpretation that the band reflects semantic distribution across frames, which is a structural property of speech, rather than misaligned processing.

### 4.3. Phase III: Decision Instability

In late layers, speech and text representations diverge in how they approach the final output. As shown in Figure 3, the best-match text layer stops increasing in late speech layers. On SpeechMMLU, even at the final speech layer, the closest text layer remains around layer 22 rather than reaching layer 28. This 6-layer gap suggests that speech representations

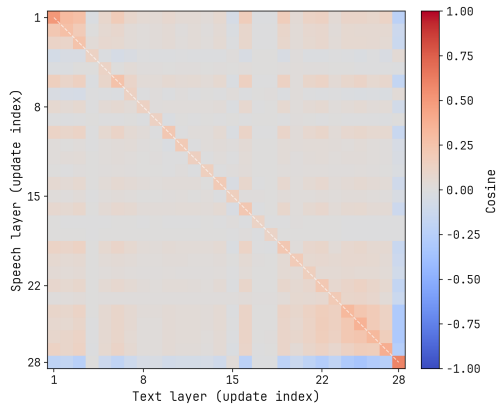


Figure 5. Cross-modal synchronization of layer-wise updates. The heatmap shows cosine similarity between speech and text update vectors at each layer. The clear diagonal pattern indicates that both modalities apply similar transformations at each layer, even though speech representations are more spread out due to redundancy.

do not complete the same late-layer processing that text undergoes. On BBH, both models get closer to the text head, with gaps of 2 layers for Qwen2.5-Omni and 1 layer for MiniCPM-o.

To understand this divergence, we examine what late layers are supposed to do. Lad et al. (2024) showed that late Transformer layers perform sharpening, where the model narrows down candidates and selects a final output token. One possibility is that speech loses the relevant information by late layers. To test this, we train linear and MLP probes on hidden states at each layer to predict the subject category on SpeechMMLU. As shown in Figure 7, probe accuracy remains high in mid and late layers, even when the model’s final S2T output is incorrect. This rules out information loss. The information is present, but the model fails to use it.

**Decision Instability in Late Layers.** Since the information is present, we next locate where the failure occurs. We first check whether speech simply has higher overall uncertainty. Figure 8 shows that the entropy of projected logits is similar for both speech and text, so global uncertainty is not

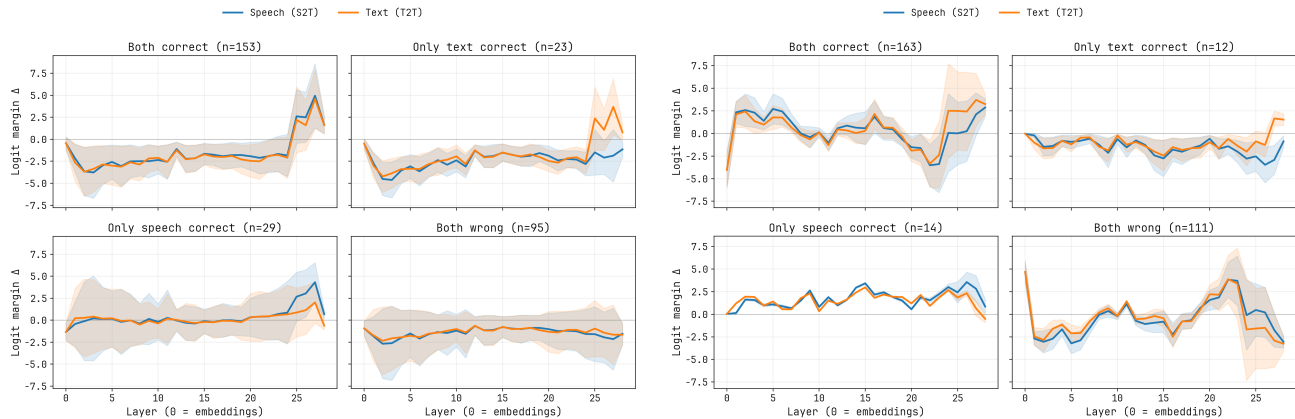


Figure 6. Layer-wise logit margin by correctness group. Left is SpeechMMLU and right is BBH. Samples are grouped by whether S2T and T2T predictions are correct. The y-axis shows the decision margin, defined as the difference between the correct answer’s logit and the strongest competitor’s logit. Positive values mean the model has separated the correct answer. For `only_t2t` cases (text correct, speech wrong), text margins become strongly positive while speech margins stay negative. Even in `only_s2t` cases where speech succeeds, speech margins reach lower peak values than text does in `only_t2t`, suggesting that speech makes less confident decisions overall.

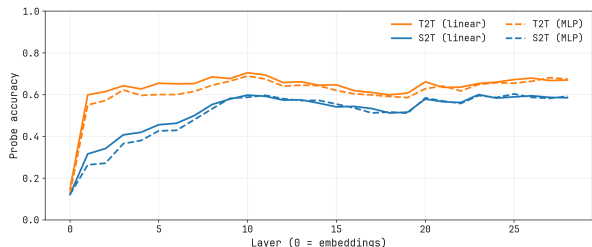


Figure 7. Layer-wise probing accuracy. Linear and MLP probes trained on hidden representations achieve high accuracy even when the final S2T output is incorrect, indicating a readout failure rather than information loss.

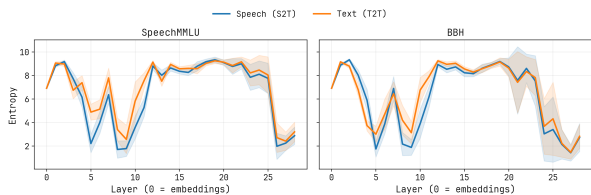


Figure 8. Layer-wise projected-logit entropy. Left is SpeechMMLU and right is BBH. The plots show the entropy of the vocabulary distribution at each layer (Logit Lens). Speech and text entropy curves are similar across both datasets, ruling out that speech is simply noisier or has higher uncertainty overall.

the issue.

To pinpoint the failure, we measure the logit margin, the difference between the correct answer’s logit and the strongest competitor’s logit. We split samples into groups based on whether text and speech give correct answers. The `only_t2t` group contains cases where text is correct but speech is wrong. Figure 6 shows that for `only_t2t` cases, text margins become positive in late layers as the model commits to the answer, while speech margins stay negative through the final layer. This is the signature of **decision instability**. Speech fails to separate the correct answer from strong competitors, because semantic information is spread across many redundant tokens and no single token carries enough signal to drive a confident decision.

### 5. Conclusion

We analyzed the modality gap in speech-language models by examining internal representations layer by layer. We identified three phases of speech processing. In Phase

I (Structural Transformation), early layers project speech features into a text-compatible space through non-linear transformation. In Phase II (Semantic Smearing), speech information spreads across many redundant tokens, creating broad alignment bands rather than sharp correspondence with text. In Phase III (Decision Instability), speech fails to separate the correct answer from competitors in late layers, even though the information is present. Our experiments show that the modality gap cannot be fixed by simple calibration or geometric alignment. Calibrating speech features at the input layer breaks the early-layer projection and causes large performance drops. The core problem is that speech tokens are individually weak. Because semantic information is distributed across many tokens, no single token carries enough signal to drive confident decisions. These findings suggest that future work should focus on reducing token redundancy rather than aligning feature distributions. Approaches like adaptive token merging or hierarchical pooling could compress distributed speech content into fewer, information-dense tokens, enabling the model to make confident decisions as it does with text.

## Impact Statement

This paper presents work whose goal is to advance the field of Machine Learning. There are many potential societal consequences of our work, none of which we feel must be specifically highlighted here.

## References

- Alain, G. and Bengio, Y. Understanding intermediate layers using linear classifier probes. In *ICLR (Workshop)*. OpenReview.net, 2017.
- Belrose, N., Furman, Z., Smith, L., Halawi, D., Ostrovsky, I., McKinney, L., Biderman, S., and Steinhardt, J. Eliciting latent predictions from transformers with the tuned lens. *CoRR*, abs/2303.08112, 2023.
- Chen, Y., Yue, X., Zhang, C., Gao, X., Tan, R. T., and Li, H. Voicebench: Benchmarking llm-based voice assistants. *CoRR*, abs/2410.17196, 2024.
- Chu, Y., Xu, J., Zhou, X., Yang, Q., Zhang, S., Yan, Z., Zhou, C., and Zhou, J. Qwen-audio: Advancing universal audio understanding via unified large-scale audio-language models. *CoRR*, abs/2311.07919, 2023.
- Chu, Y., Xu, J., Yang, Q., Wei, H., Wei, X., Guo, Z., Leng, Y., Lv, Y., He, J., Lin, J., Zhou, C., and Zhou, J. Qwen2-audio technical report. *CoRR*, abs/2407.10759, 2024.
- Cui, W., Yu, D., Jiao, X., Meng, Z., Zhang, G., Wang, Q., Guo, S. Y., and King, I. Recent advances in speech language models: A survey. In *ACL (1)*, pp. 13943–13970. Association for Computational Linguistics, 2025.
- Dorszewski, T., Jacobsen, A. K., Tetková, L., and Hansen, L. K. How redundant is the transformer stack in speech representation models? In *ICASSP*, pp. 1–5. IEEE, 2025.
- Fang, Q., Guo, S., Zhou, Y., Ma, Z., Zhang, S., and Feng, Y. Llama-omni: Seamless speech interaction with large language models. In *ICLR*. OpenReview.net, 2025a.
- Fang, Y., Sun, H., Liu, J., Zhang, T., Zhou, Z., Chen, W., Xing, X., and Xu, X. S2sbench: A benchmark for quantifying intelligence degradation in speech-to-speech large language models. *CoRR*, abs/2505.14438, 2025b.
- Geva, M., Schuster, R., Berant, J., and Levy, O. Transformer feed-forward layers are key-value memories. In *EMNLP (1)*, pp. 5484–5495. Association for Computational Linguistics, 2021.
- Glazer, N., Segal-Feldman, Y., Segev, H., Shamsian, A., Buchnick, A., Hetz, G., Fetaya, E., Keshet, J., and Navon, A. Beyond transcription: Mechanistic interpretability in ASR. *CoRR*, abs/2508.15882, 2025.
- Goel, A., Ghosh, S., Kim, J., Kumar, S., Kong, Z., Lee, S., Yang, C. H., Duraiswami, R., Manocha, D., Valle, R., and Catanzaro, B. Audio flamingo 3: Advancing audio intelligence with fully open large audio language models. *CoRR*, abs/2507.08128, 2025.
- Hendrycks, D., Burns, C., Basart, S., Zou, A., Mazeika, M., Song, D., and Steinhardt, J. Measuring massive multitask language understanding. In *ICLR*. OpenReview.net, 2021.
- Lad, V., Gurnee, W., and Tegmark, M. The remarkable robustness of llms: Stages of inference? *CoRR*, abs/2406.19384, 2024.
- Liang, W., Zhang, Y., Kwon, Y., Yeung, S., and Zou, J. Y. Mind the gap: Understanding the modality gap in multimodal contrastive representation learning. In *NeurIPS*, 2022.
- Liu, W., Chen, Q., Wang, W., Chen, Y., Xu, J., Guo, Z., Yang, G., Li, W., Yang, X., Jin, T., Fang, M., Zuo, J., Jionghao, B., and Liu, Z. Speech token prediction via compressed-to-fine language modeling for speech generation, 2025. URL <https://arxiv.org/abs/2505.24496>.
- Ma, Y., Sang, J., and Li, R. Behind the scenes: Mechanistic interpretability of lora-adapted whisper for speech emotion recognition. *CoRR*, abs/2509.08454, 2025.
- Meng, K., Bau, D., Andonian, A., and Belinkov, Y. Locating and editing factual associations in GPT. In *NeurIPS*, 2022.
- Mousavi, P., Wang, Y., Ravanelli, M., and Subakan, C. ALAS: measuring latent speech-text alignment for spoken language understanding in multimodal llms. *CoRR*, abs/2505.19937, 2025.
- nostalgebraist. Interpreting GPT: the logit lens. <https://www.lesswrong.com/posts/AcKRB8wDpdaN6v6ru/interpreting-gpt-the-logit-lens>, 2020. Accessed: 2025-01-23.
- Park, K., Choe, Y. J., and Veitch, V. The linear representation hypothesis and the geometry of large language models. In *ICML*. OpenReview.net, 2024.
- Suzgun, M., Scales, N., Schärli, N., Gehrmann, S., Tay, Y., Chung, H. W., Chowdhery, A., Le, Q. V., Chi, E. H., Zhou, D., and Wei, J. Challenging big-bench tasks and whether chain-of-thought can solve them. In *ACL (Findings)*, pp. 13003–13051. Association for Computational Linguistics, 2023.
- Team, C., Zhang, D., Wang, G., Xue, J., Fang, K., Zhao, L., Ma, R., Ren, S., Liu, S., Guo, T., Zhuang, W., Zhang,

- X., Song, X., Yan, Y., He, Y., Cici, Shen, B., Zhu, C., Ma, C., Chen, C., Chen, H., Li, J., Li, L., Zhu, M., Li, P., Wang, Q., Deng, S., Xiong, W., Huang, W., Yang, W., Jiang, Y., Yang, Y., Tian, Y., Ma, Y., Yu, Y., Zhang, Z., Yue, Z., Xiao, B., Xia, B., Gao, B., Ye, B., Cai, C., Liu, C., He, C., Li, C., Zhu, D., Zhang, D., Shi, F., Wang, G., Zhang, H., Lv, H., Li, H., Tian, H., Qu, H., Xu, H., Zhang, H., Liu, H., Duo, J., Zuo, J., Wei, J., Xiao, J., Dong, J., Shi, J., Hu, J., Bao, K., Zhou, K., Zhang, L., Chen, M., Chen, N., Zhang, P., Chen, Q., Wang, Q., Li, R., Liu, S., Wang, S., Li, S., Yu, S., Cao, S., Chen, S., Gu, S., Wang, W., Ma, W., Deng, X., Yong, X., Zhang, X., Wang, X., Song, Y., Zhao, Y., Zhao, Y., Gao, Y., Cheng, Y., Tu, Y., Wang, Y., Huang, Z., Tang, Z., Lin, Z., Song, Z., Xu, Z., Zheng, Z., and Jiang, Z. MIMO-audio: Audio language models are few-shot learners, 2025. URL <https://arxiv.org/abs/2512.23808>.
- Wang, C., Lu, H., Zhang, X., Liu, S., Lu, Y., Li, J., and Wu, Z. Closing the modality reasoning gap for speech large language models, 2026. URL <https://arxiv.org/abs/2601.05543>.
- Xiang, B., Zhao, S., Guo, T., and Zou, W. Understanding the modality gap: An empirical study on the speech-text alignment mechanism of large speech language models. *CoRR*, abs/2510.12116, 2025.
- Xu, J., Guo, Z., He, J., Hu, H., He, T., Bai, S., Chen, K., Wang, J., Fan, Y., Dang, K., Zhang, B., Wang, X., Chu, Y., and Lin, J. Qwen2.5-omni technical report. *CoRR*, abs/2503.20215, 2025.
- Yang, Z., Shimizu, S., Yu, Y., and Chu, C. When large language models meet speech: A survey on integration approaches. In *ACL (Findings)*, pp. 20298–20315. Association for Computational Linguistics, 2025.
- Yao, Y., Yu, T., Zhang, A., Wang, C., Cui, J., Zhu, H., Cai, T., Li, H., Zhao, W., He, Z., Chen, Q., Zhou, H., Zou, Z., Zhang, H., Hu, S., Zheng, Z., Zhou, J., Cai, J., Han, X., Zeng, G., Li, D., Liu, Z., and Sun, M. Minicpm-v: A GPT-4V level MLLM on your phone. *CoRR*, abs/2408.01800, 2024.
- You, K. Semantics at an angle: When cosine similarity works until it doesn't. *CoRR*, abs/2504.16318, 2025.
- Zhang, D., Li, S., Zhang, X., Zhan, J., Wang, P., Zhou, Y., and Qiu, X. Speechgpt: Empowering large language models with intrinsic cross-modal conversational abilities. In *EMNLP (Findings)*, pp. 15757–15773. Association for Computational Linguistics, 2023.
- Zuo, J., Zhang, G., Fang, M., Ji, S., Jiao, X., Li, J., Guo, Y., and Zhao, Z. Entropy-based coarse and compressed semantic speech representation learning. *CoRR*, abs/2509.00503, 2025.

## Appendix

### A. Robustness of Structural Alignment

This section presents sensitivity analyses to verify that the three-phase structure, namely Structural Transformation, Semantic Smearing, and Decision Instability, is a robust property of the model and not an artifact of specific alignment hyperparameters.

#### A.1. DTW Sensitivity and Band Statistics

The cross-layer alignment analysis in Section 3.3 relies on DTW to find the best-match path between speech and text hidden states. This section verifies that the extracted paths are not artifacts of specific hyperparameter choices.

**Setup.** The DTW base layer  $\ell_0$  is swept over 0, 5, 10, and 20. This parameter controls which layer is used as the reference for computing cross-layer similarity. The score metric is varied between cosine similarity and normalized  $L_2$  distance, and an optional Sakoe-Chiba band constraint is applied. For each configuration, two statistics are computed on the resulting alignment path. Path linearity, measured by  $R^2$  from a linear fit, indicates how close the path is to a diagonal. A diagonal path means speech layer  $i$  aligns with text layer  $i$ , i.e., both modalities process information at a similar pace. Stall fraction measures the proportion of horizontal steps in the path, indicating how often multiple speech layers map to the same text layer.

**Results.** When the base layer is set to 0, path linearity drops substantially, especially for SpeechMMLU under cosine scoring. In contrast, base layers 5 and above yield stable, near-diagonal paths across all metric and constraint combinations. This confirms that the alignment structure reported in the main text is robust and not sensitive to hyperparameter choices. The instability at layer 0 is consistent with the interpretation that early layers form a heterogeneous projection zone where speech representations have not yet converged to a text-like geometry.

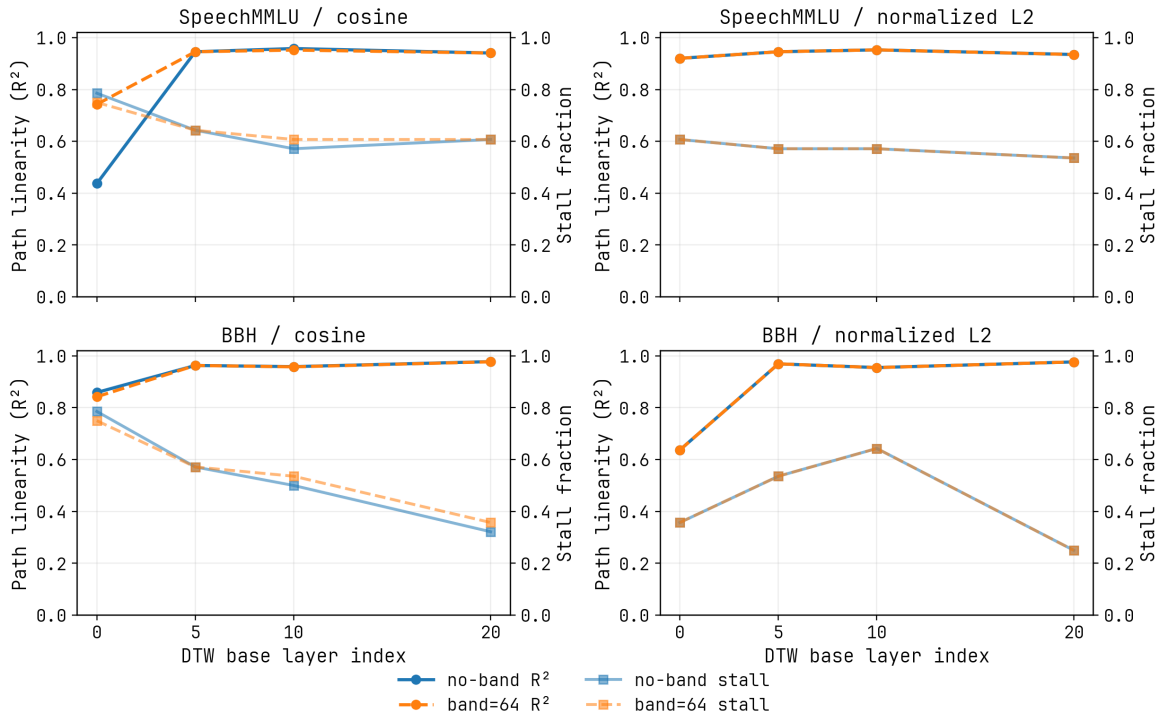


Figure 9. DTW sensitivity sweep. Path linearity is reported via  $R^2$  and stagnation via stall fraction. Base layer 0 is notably less stable, while base layers 5 and above yield near-diagonal paths with a consistent late-layer plateau.

## B. Supplementary Calibration Results on SpeechMMLU

To assess generalization across benchmarks, we replicate the mean and standard deviation calibration experiment on SpeechMMLU for Qwen2.5-Omni using the same three conditions as Table 1. The primary finding is that input-level calibration at layer 0 again produces a large accuracy drop, from 70.2% to 23.0%. This replication strengthens the main-text conclusion that the early-layer modality gap cannot be closed by a simple affine alignment of first-order statistics.

**Important caveat for review.** The *last-layer* condition carries two confounds that limit its interpretability on this benchmark. First, the affine transform is applied at the final LayerNorm input whenever audio is present, so it modifies the full token sequence rather than only the audio-token span. Second, SpeechMMLU evaluation extracts answers by parsing a short generated string into an option index, making it sensitive to formatting changes. Together, these factors cause the unparseable-output rate to rise from 0.27% at baseline to 42.60% under last-layer calibration, even when partial semantic content may be preserved. We therefore report the last-layer result for completeness but treat it as a supplementary observation rather than a controlled causal test.

Method	SpeechMMLU Accuracy	$\Delta$ vs Baseline
None (baseline)	70.2%	—
Input (layer 0)	23.0%	-47.2%
Output (last layer)	42.4%	-27.8%

Table 4. Mean and std calibration on SpeechMMLU. Input-level calibration collapses accuracy, consistent with the BBH result. Last-layer calibration is confounded by format-sensitive parsing as discussed in the text.

**Takeaway.** The input-level collapse observed on both BBH and SpeechMMLU indicates that naive first-moment matching disrupts the heterogeneous projection stage in early layers, supporting the claim that the modality gap reflects a structural mismatch rather than a correctable distribution shift.

## C. Token Merging Experiment

Our analysis identifies two mechanisms by which speech’s inherent redundancy may impair performance. In Phase II (Semantic Smearing), semantic information spreads across many tokens, creating broad alignment bands rather than sharp correspondence with text. In Phase III (Decision Instability), the per-token signal is too weak to drive confident late-layer sharpening. The causal intervention in Table 3 confirms that artificially increasing redundancy in text degrades accuracy, supporting the hypothesis that redundant tokens dilute decision evidence. These findings motivate exploring whether reducing redundancy at inference time can partially mitigate the speech modality gap.

We implement a simple KV token merging scheme on Qwen2.5-Omni in the S2T setting. At each layer within a specified range, we compute pairwise cosine similarity among key vectors and merge tokens whose similarity exceeds a threshold of 0.90, up to a maximum merge fraction per layer. The layer range starts at layer 7 to avoid interfering with Phase I structural transformation and extends to layers 15, 18, or 21 (end-exclusive). The maximum merge fraction is set to 0.10, 0.20, or 0.25. All runs use seed 0 with 1000 samples per benchmark.

Table 5 reports the results. Most configurations yield small improvements on both benchmarks. BBH shows more consistent gains, with the 7-to-21 range achieving up to +0.5 percentage points. SpeechMMLU improvements are smaller and more variable across settings. These observations are consistent with the hypothesis that reducing token redundancy can help late-layer decision-making, though the effect sizes are modest. We emphasize that this is a preliminary sweep rather than a controlled causal study, and the gains may partly reflect task-specific factors. Nevertheless, the results provide supportive evidence for the direction suggested in Section 5, namely that adaptive token merging or hierarchical pooling could compress distributed speech content into fewer, information-dense tokens.

## D. Additional Deep Diagnostics for MiniCPM-o

The projected-logit entropy, layer-wise decision margin, and norm-control suite are replicated for MiniCPM-o on SpeechMMLU and VoiceBench BBH using 300 items per dataset with seed 0 and 4-bit quantization.

## Anatomy of the Modality Gap: Dissecting the Internal States of End-to-End Speech LLMs

Key cos thr	Layers (start–end)	Max frac	SpeechMMLU Acc.	$\Delta$	BBH Acc.	$\Delta$
Baseline (no merge)			62.6%	–	59.8%	–
0.90	7–15	0.10	<b>63.1%</b>	<b>+0.5</b>	<b>60.1%</b>	<b>+0.3</b>
0.90	7–15	0.20	<b>63.1%</b>	<b>+0.5</b>	<b>60.2%</b>	<b>+0.4</b>
0.90	7–15	0.25	<b>63.1%</b>	<b>+0.5</b>	<b>60.2%</b>	<b>+0.4</b>
0.90	7–18	0.10	<b>62.7%</b>	<b>+0.1</b>	<b>59.9%</b>	<b>+0.1</b>
0.90	7–18	0.20	<b>62.7%</b>	<b>+0.1</b>	59.6%	-0.2
0.90	7–18	0.25	<b>62.7%</b>	<b>+0.1</b>	59.6%	-0.2
0.90	7–21	0.10	<b>63.1%</b>	<b>+0.5</b>	<b>60.3%</b>	<b>+0.5</b>
0.90	7–21	0.20	<b>63.1%</b>	<b>+0.5</b>	<b>60.3%</b>	<b>+0.5</b>
0.90	7–21	0.25	<b>63.1%</b>	<b>+0.5</b>	<b>60.3%</b>	<b>+0.5</b>

Table 5. **KV token merging sweep on SpeechMMLU and VoiceBench BBH.** Tokens with key cosine similarity above 0.90 are merged up to a maximum fraction per layer, applied to the specified layer range. Most configurations yield modest improvements over the no-merge baseline, with BBH showing more consistent gains. Deltas are in percentage points.

### D.1. Projected-Logit Entropy

Across both datasets, speech and text entropy curves largely overlap through the depth of the model, with both modalities showing the same late-layer entropy collapse. This indicates that MiniCPM-o’s S2T failures are not explained by a globally noisier, higher-entropy distribution in speech. The results are consistent with the findings in Section 4. This motivates focusing on option-level separation rather than overall uncertainty. Figure 10 provides the corresponding layer-wise entropy trajectories.

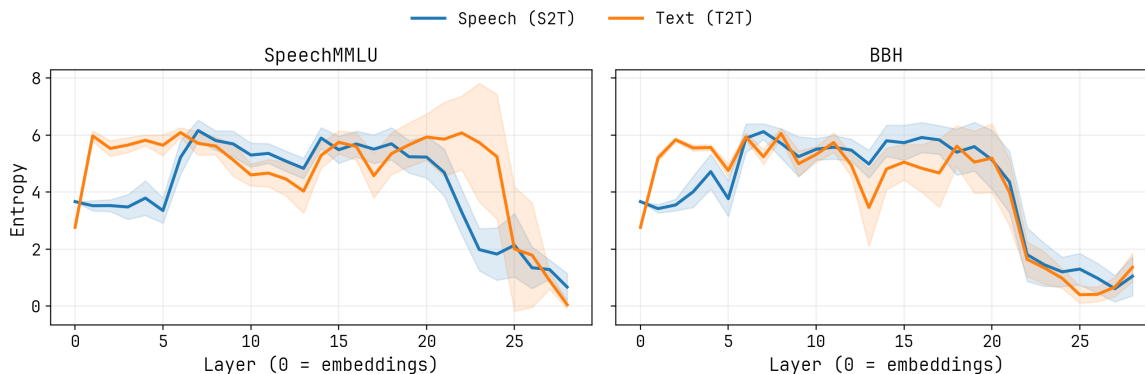


Figure 10. **MiniCPM-o layer-wise projected-logit entropy.** Speech and text show comparable entropy trajectories across layers, suggesting the modality gap is not driven by uniformly higher uncertainty.

### D.2. Decision Instability via Layer-wise Margin

The `only_t2t` group shows a clear late-layer divergence. Text margins grow positive as the model commits, whereas speech margins stay near zero or negative. Even when both modalities are correct, speech margins are typically smaller, consistent with weaker late-layer sharpening under speech input. Figure 11 shows the full groupwise margin curves.

### D.3. Norm Control Analysis for Pre-LN and Post-LN

Pre-LN residual norms can drift in late layers, but the post-LN stream fed into attention remains closely matched between modalities. This mirrors the Qwen2.5-Omni pattern and suggests that the modality gap is not a trivial norm or scale mismatch after normalization. Figure 12 reports the norm-control results.

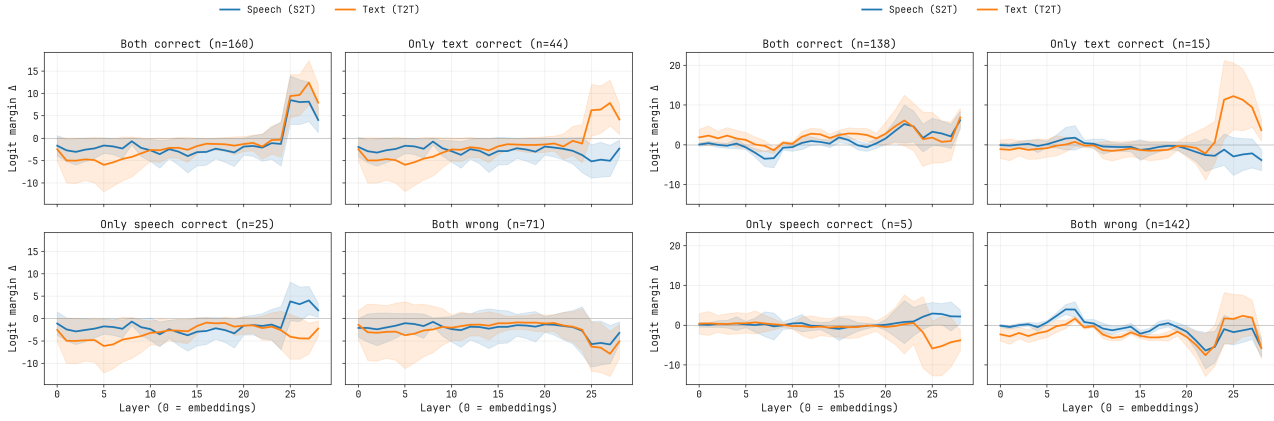


Figure 11. MiniCPM-o layer-wise logit margin by correctness group. Left is SpeechMMLU and right is BBH. For `only_t2t` samples, text margins become positive in late layers while speech margins often remain negative, consistent with last-mile decision instability.

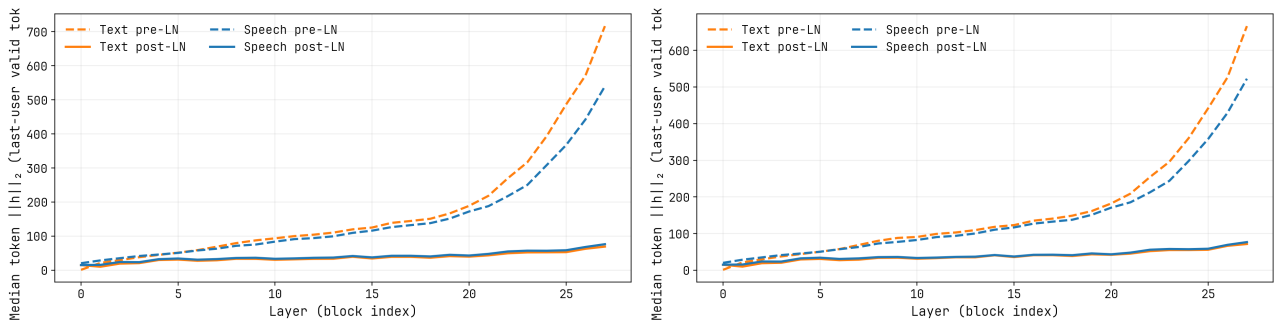


Figure 12. MiniCPM-o pre-LN and post-LN norms. Left is SpeechMMLU and right is BBH. As in Qwen2.5-Omni, post-LN norms are comparatively stable across modalities, ruling out simple scaling mismatch as the primary explanation.

## E. Generalization to LLaMA-Omni

To test whether these findings are specific to Qwen2.5-Omni, the core diagnostics are replicated on **LLaMA-Omni**, which has 33 layers and hidden dimension 4096.

### E.1. Structural Alignment via CKA

Both tasks exhibit a clear early-layer low-similarity zone, suggesting that the Structural Transformation phase is not unique to Qwen2.5-Omni but may be common in end-to-end speech adapters. The early low-similarity region persists across both datasets, indicating that speech representations are not immediately text-like even in this different backbone. Compared to Qwen2.5-Omni, the alignment band is weaker and more compressed, consistent with a less reliable cross-modal geometry. Figure 13 shows the cross-layer CKA heatmaps.

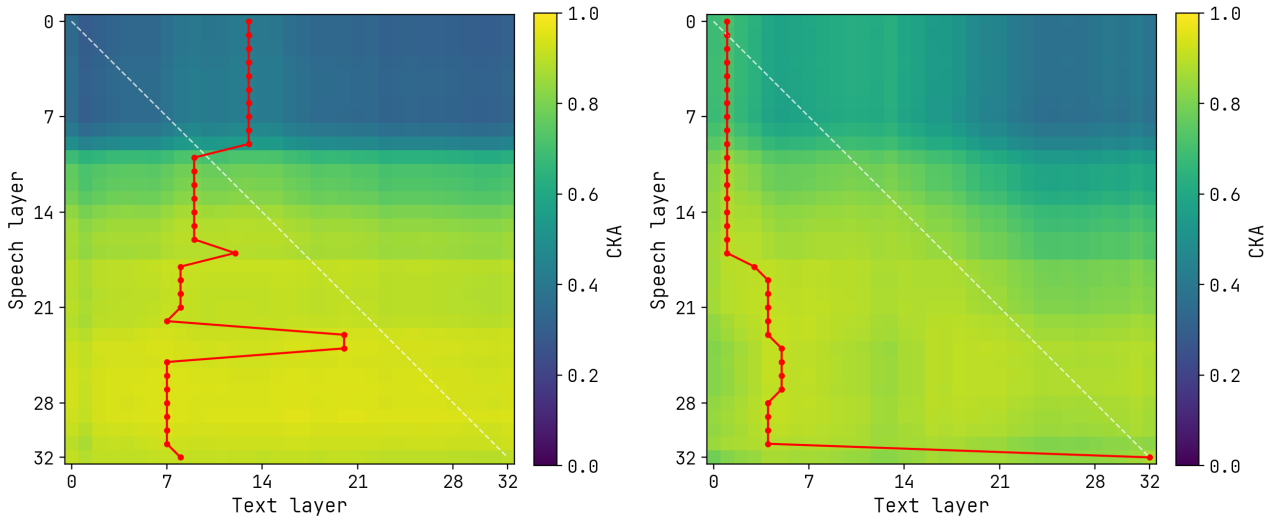


Figure 13. **LLaMA-Omni cross-layer CKA heatmaps.** Left is BBH and right is SpeechMMLU. Both tasks show an early low-similarity zone, consistent with heterogeneous projection.

### E.2. Projected-Logit Entropy

Entropy trends are broadly aligned between modalities, so the gap is unlikely to be driven by uniformly elevated uncertainty in speech. This again points to option-separation failure or decision instability rather than a global confidence collapse. Figure 14 provides the entropy curves.

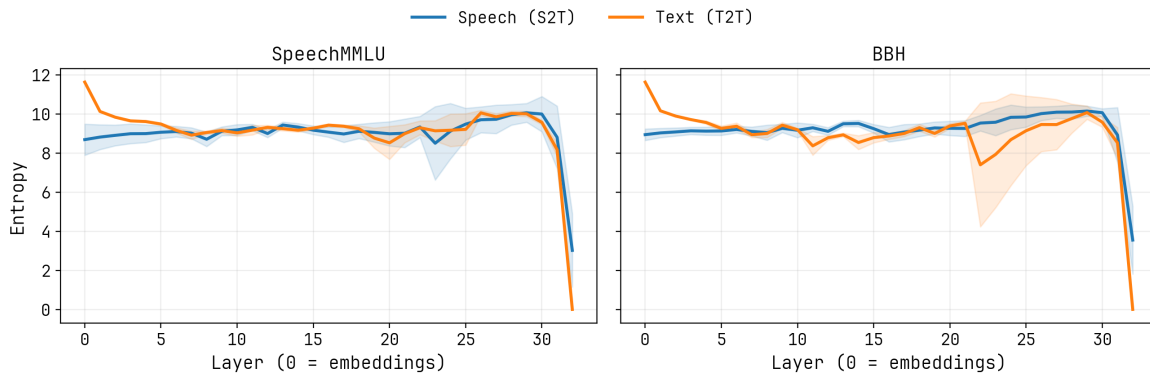


Figure 14. **LLaMA-Omni layer-wise projected-logit entropy.** Entropy curves are comparable across modalities, indicating that failures are not explained by uniformly higher global uncertainty in speech.

### E.3. Decision Instability via Layer-wise Margin

As with Qwen2.5-Omni, late-layer margins in the `only_t2t` group are systematically weaker and often negative for speech, indicating failure to sharpen onto the correct option. The effect is attenuated on BBH relative to SpeechMMLU, consistent with task-dependent decision stability. Figure 15 shows the groupwise margin trajectories.

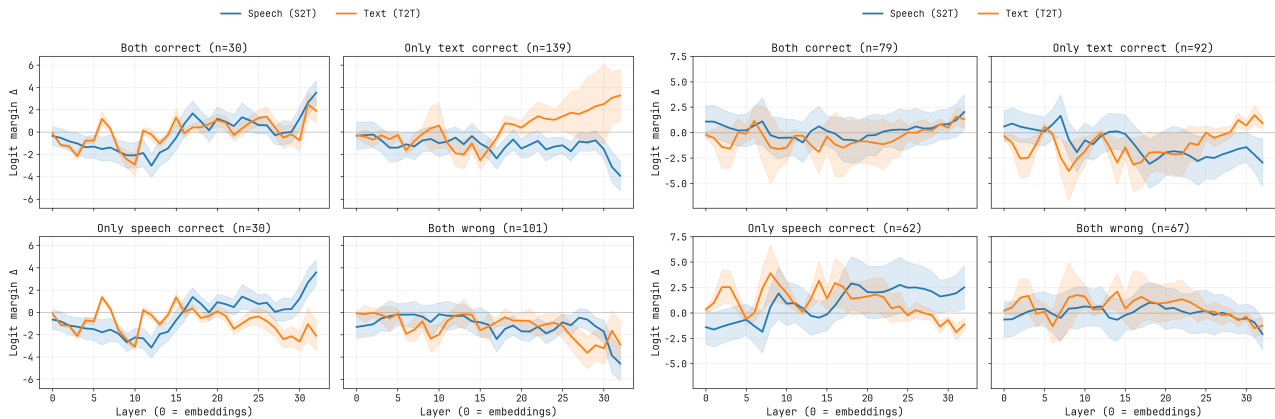


Figure 15. LLaMA-Omni layer-wise logit margin by correctness group. Left is SpeechMMLU and right is BBH. The `only_t2t` group exhibits weaker, often negative, speech margins in late layers, consistent with last-mile decision instability.

### E.4. Norm Control Analysis

Despite large pre-LN residual growth in late layers, post-LN norms remain tightly coupled between speech and text. A simple distribution-scale mismatch after normalization is therefore unlikely to explain the observed decision failures. Figure 16 provides the norm-control visualizations.

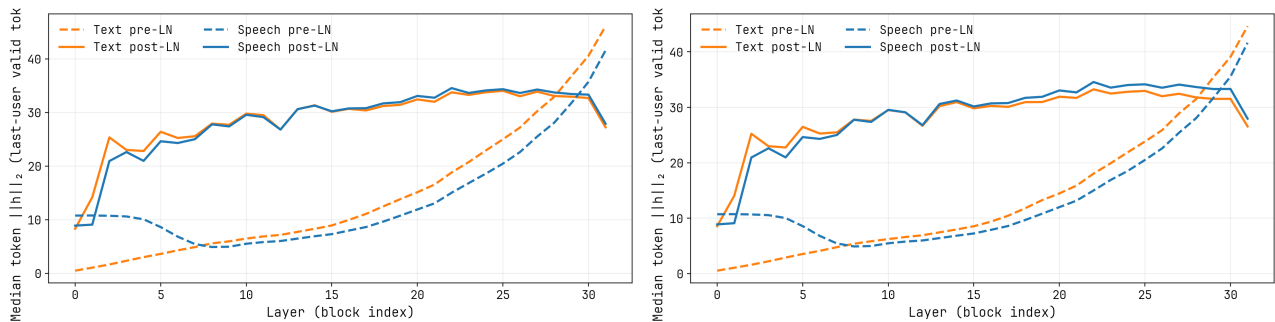


Figure 16. LLaMA-Omni pre-LN and post-LN norms. Left is SpeechMMLU and right is BBH. Post-LN norms are comparatively stable across modalities, suggesting that decision failures are not caused by a simple scale mismatch.

## F. Failure Analysis of Qwen2-Audio

**Qwen2-Audio** is evaluated to understand the failure mode of a model that performs near chance on SpeechMMLU while showing a smaller, though still substantial, gap on BBH. This contrast helps distinguish between two qualitatively different failure modes. In Qwen2.5-Omni and MiniCPM-o, the primary bottleneck is Decision Instability, meaning speech representations achieve reasonable alignment with text geometry but fail to sharpen onto the correct answer in late layers. In Qwen2-Audio, the failure is more fundamental. CKA heatmaps reveal uniformly low cross-modal similarity across all layers, indicating that speech representations never properly align with text geometry at any stage of processing. We term this pattern *Representation Failure* to distinguish it from the Phase III Decision Instability observed in better-performing models.

**F.1. Structural Alignment**

Unlike Qwen2.5-Omni and MiniCPM-o, Qwen2-Audio does not exhibit a clear diagonal or broad middle-layer band in its CKA heatmap. Instead, the best-match path collapses toward a near-vertical trajectory that maps many speech layers to the same late text layer. This suggests a degenerate alignment regime where speech representations fail to track the text processing trajectory. Figure 17 visualizes this degenerate cross-modal alignment.

**Uniformly low CKA across layers.** The key diagnostic observation is that Qwen2-Audio shows low CKA values not just in early layers, as expected from Phase I Structural Transformation, but across the entire layer range. In Qwen2.5-Omni and MiniCPM-o, CKA heatmaps exhibit a pronounced high-similarity band in middle layers where speech and text representations converge. Qwen2-Audio lacks this band entirely. The absence of any layer range with strong cross-modal alignment suggests that speech representations in this model occupy a fundamentally different region of representational space from text, never achieving the geometric correspondence that enables successful downstream processing.

**Task-dependent impact.** This Representation Failure explains the asymmetric performance degradation across tasks. SpeechMMLU is a knowledge-dense task that requires precise semantic representations to query factual knowledge stored in FFN weights. Recent work has characterized FFN layers as key-value memory stores where input representations act as retrieval keys (Geva et al., 2021; Meng et al., 2022). When speech representations fail to align with the text geometry that the model was trained on, they cannot properly trigger the correct memory patterns in FFN layers. The result is near-chance performance because the factual knowledge is inaccessible to misaligned representations. BBH, by contrast, is a reasoning task that depends more on compositional manipulation of intermediate representations and less on precise factual recall. Even with imperfect alignment, some reasoning patterns may remain partially accessible, explaining the smaller but still significant performance gap on this benchmark.

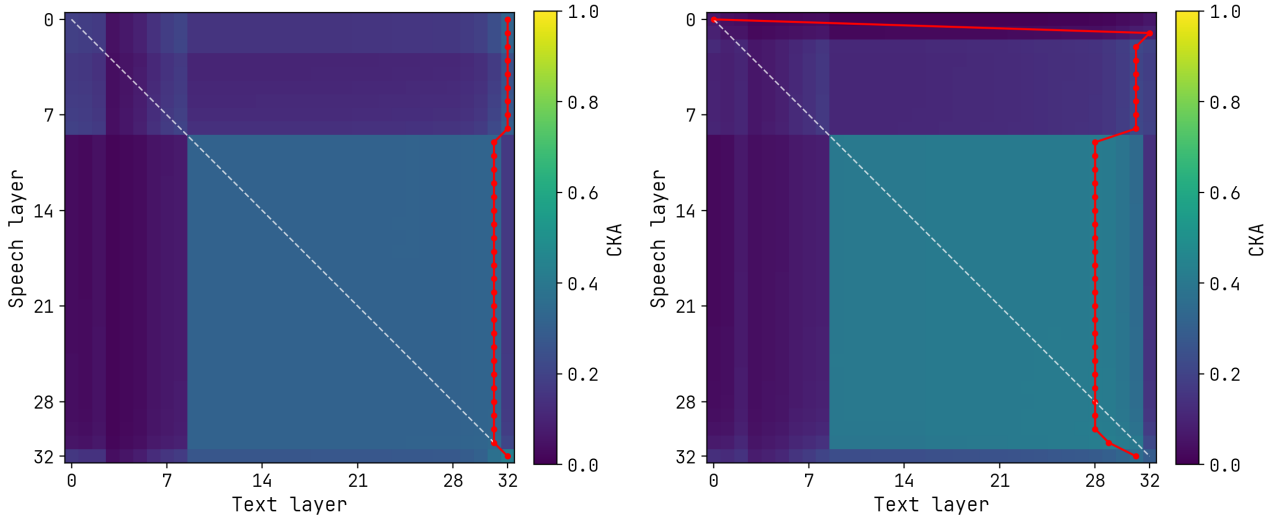


Figure 17. **Qwen2-Audio cross-layer CKA heatmaps.** Left is BBH and right is SpeechMMLU. Unlike Qwen2.5-Omni and MiniCPM-o, there is no high-similarity diagonal band in middle layers, indicating that speech representations never converge to text-like geometry.

**Interpretation.** The CKA analysis suggests that Qwen2-Audio’s failure mode is qualitatively different from the Decision Instability observed in Qwen2.5-Omni and MiniCPM-o. Those models achieve reasonable cross-modal alignment in middle layers but fail to maintain stable decisions in late layers. Qwen2-Audio fails at a more fundamental level. Speech representations never enter the text-aligned subspace where the model’s knowledge and reasoning capabilities reside. This Representation Failure is a prerequisite failure, preventing even Phase II and Phase III processing from operating on well-formed inputs. The task-dependent severity, with SpeechMMLU showing near-chance performance while BBH retains partial functionality, is consistent with the interpretation that knowledge retrieval is more sensitive to precise representational alignment than logical reasoning.

### F.2. Semantic Accessibility via Logit Lens

On SpeechMMLU, text begins to concentrate probability mass onto the correct option in late layers, whereas speech remains near the chance-level baseline and does not reliably elevate the correct option above competitors. On BBH the curves hover near 0.5 with high variance in late layers, indicating unstable option separation rather than consistent late-layer sharpening. Figure 18 provides the candidate-only semantic accessibility curves.

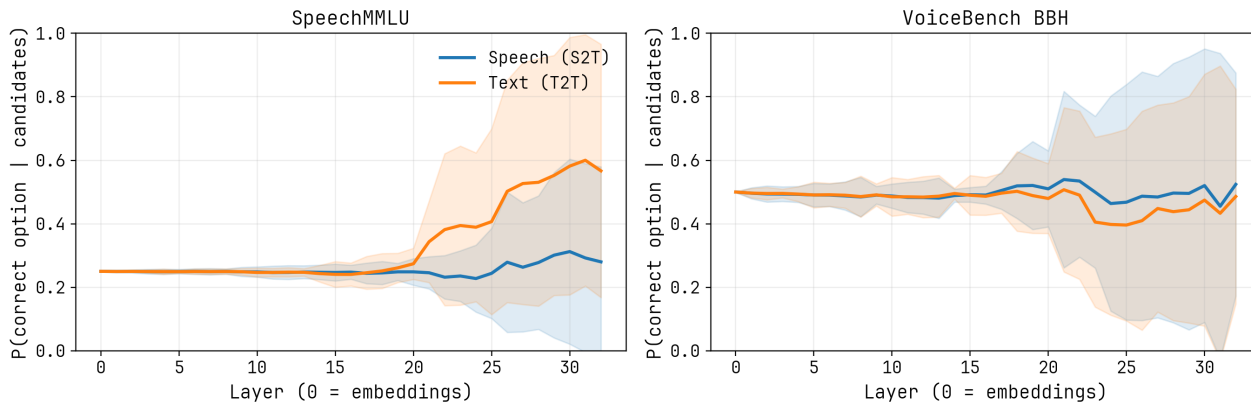


Figure 18. **Qwen2-Audio semantic accessibility via candidate-only logit lens.** Per-layer probability of the correct answer option among candidates for S2T and T2T at the decision prefix. Speech fails to elevate the correct option, especially on SpeechMMLU.

### F.3. Projected-Logit Entropy

Entropy remains comparable across modalities through most layers and collapses only very late, indicating that the model is not globally uncertain in speech. In SpeechMMLU, speech entropy tends to decrease later than text, consistent with delayed or incomplete late-layer sharpening under speech input. Figure 19 shows the layer-wise entropy trajectories for Qwen2-Audio.

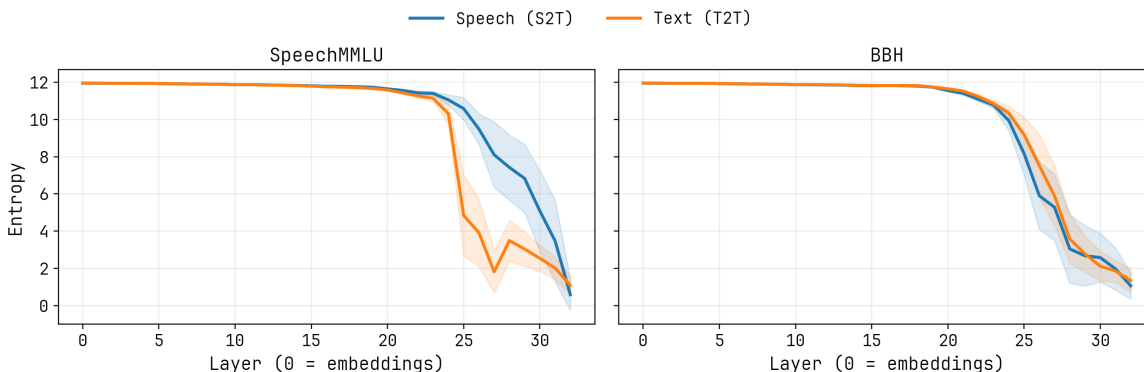


Figure 19. **Qwen2-Audio layer-wise projected-logit entropy.** Global uncertainty is not uniformly higher for speech across layers, suggesting the failure is not simply more uncertainty but a downstream decision or readout issue.

### F.4. Decision Margin via Layer-wise Margin by Correctness Group

For the `only_t2t` group, text margins become strongly positive in late layers, while speech margins stay negative and often decrease further. This indicates a failure to separate the correct option. The existence of `only_s2t` cases shows that Qwen2-Audio can occasionally form the correct decision, but does so with weaker and less stable margins. Figure 20 provides the groupwise margin curves.

## Anatomy of the Modality Gap: Dissecting the Internal States of End-to-End Speech LLMs

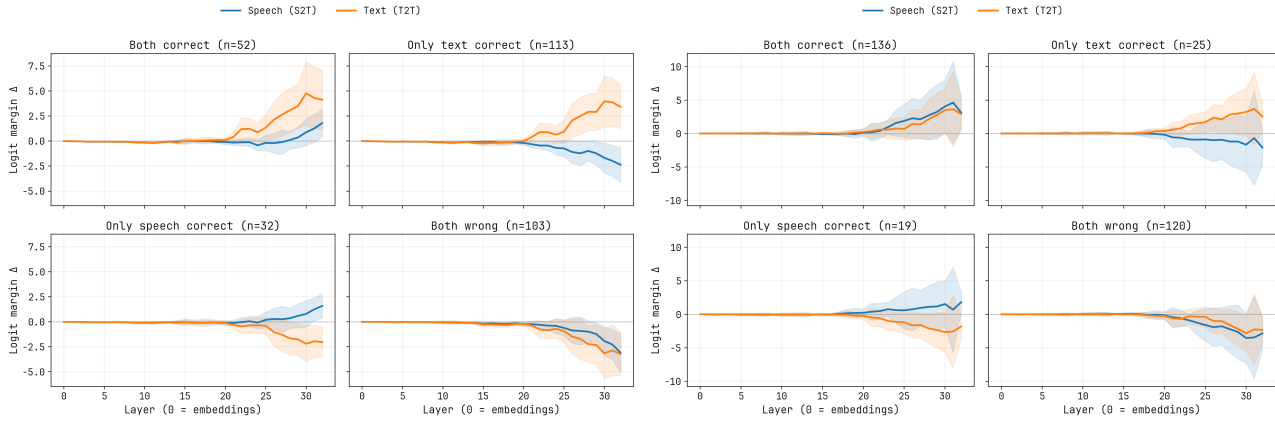


Figure 20. Qwen2-Audio layer-wise logit margin by correctness group. Left is SpeechMMLU and right is BBH. Margin trajectories provide a complementary view of why S2T answers fail even when intermediate representations are partially informative.

### F.5. Norm Control Analysis for Pre-LN and Post-LN

Pre-LN norms diverge substantially in late layers, but post-LN norms, i.e., the normalized stream entering attention, remain tightly aligned across modalities. The failure mode is therefore not a simple amplitude mismatch. It is more consistent with representational or decision readout failure. Figure 21 shows the pre-LN and post-LN norm controls for Qwen2-Audio.

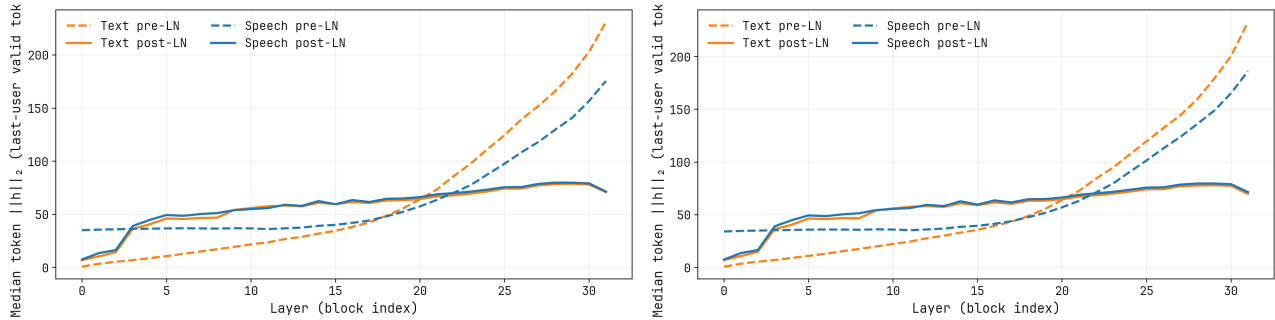


Figure 21. Qwen2-Audio pre-LN and post-LN norms. Left is SpeechMMLU and right is BBH. Post-LN norms remain comparatively stable, indicating that scaling alone is not a sufficient explanation of failure.

## G. Qualitative Case Studies

To visualize the nature of the modality gap, specific examples are presented where the model correctly answers the text query but fails on the speech query.

**Setup.** Instances are selected with matched prompts where T2T is correct but S2T is incorrect. The per-layer probability assigned to the ground-truth option among the answer candidates at the decision prefix is visualized. This view isolates whether the correct answer becomes a plausible competitor during intermediate computation, or whether it never gains probability mass under speech.

**Results.** In SpeechMMLU cases, both modalities can transiently elevate the correct option, but speech trajectories are noticeably more unstable in the late layers and can fail to maintain the correct option as the top choice. In BBH cases, text shows a clean monotonic rise toward a near-deterministic correct decision, whereas speech stays low and noisy. This indicates a failure of late-layer sharpening even when the correct option is present in the candidate set. Table 6 and Figure 22 summarize the selected prompts and the corresponding per-layer traces.

Table 6. **Qualitative cases (text correct, speech wrong).** We show prompts for selected instances where T2T answers correctly but S2T fails. The accompanying figure plots the per-layer probability of the correct option among answer candidates (logit-lens, option-only normalization).

Dataset	Item	Prompt (truncated)
SpeechMMLU	anatomy_1	Question: A "dished face" profile is often associated with Option A: a protruding mandible due to reactivation of the condylar cartilage by acromegaly. Option B: a recessive maxil...
SpeechMMLU	anatomy_11	Question: A patient suffers damage to the orbit in a road traffic incident resulting in damage to the third cranial nerve. Which of the following signs will be present? Option A:...
BBH	bbh_hyperbaton_105	Which sentence has the correct adjective order: Options: (A) repulsive normal-size green old-fashioned cardboard surfboard (B) repulsive normal-size old-fashioned green cardboard...
BBH	bbh_hyperbaton_111	Which sentence has the correct adjective order: Options: (A) little black driving ship (B) driving little black ship. Think step by step, and when you provide the final answer, pl...

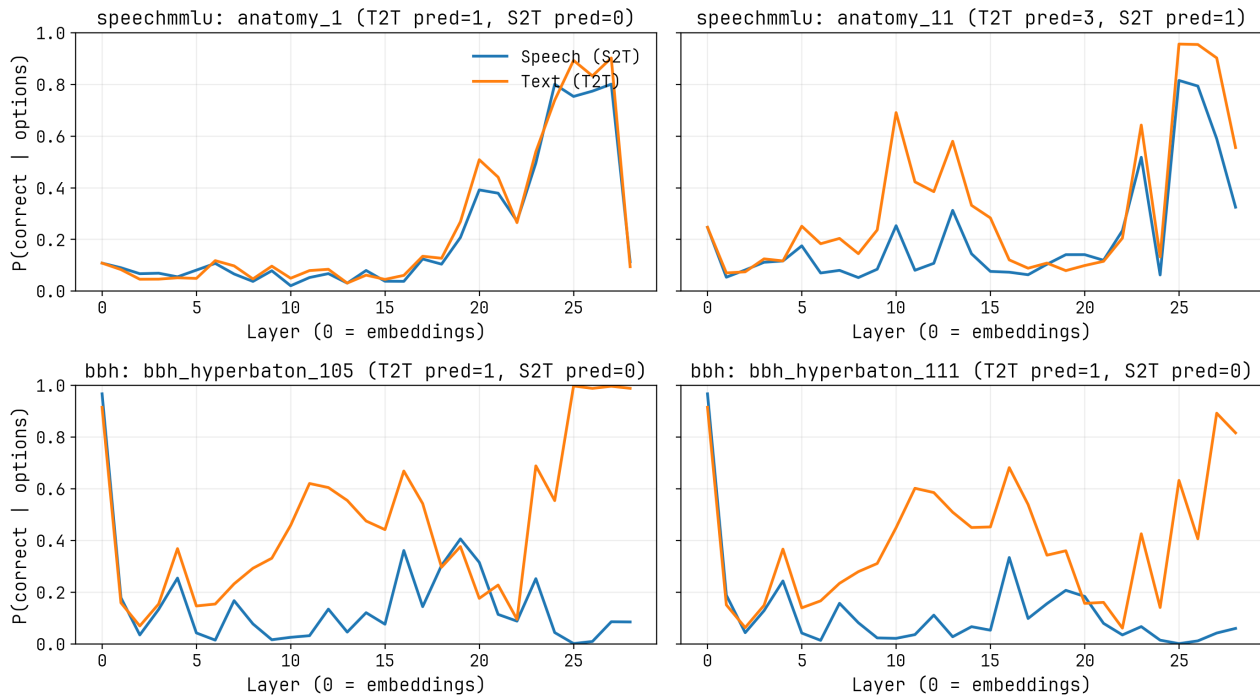


Figure 22. **Qualitative logit-trace case studies for text-correct and speech-wrong instances.** Per-layer probability of the correct answer option among candidates for S2T and T2T on the same instance. Text confidence rises and stabilizes in late layers, while speech remains unstable or diverges.

## H. Limitations and Future Work

This work is primarily diagnostic rather than prescriptive. Our goal is to characterize the mechanisms underlying the speech-to-text modality gap, not to propose a complete engineering solution. The interventions we employ, such as mean and standard deviation calibration, artificial text redundancy injection, and KV token merging, are designed to validate specific hypotheses about the three-phase structure rather than to serve as practical remedies. We view this diagnostic framing as a necessary foundation for future work that targets the root causes of speech underperformance.

A key methodological limitation concerns the causal experiment in Table 3, where we inject redundancy into text by repeating each word multiple times. This artificial redundancy is discrete and symbol-level, whereas speech redundancy arises from continuous acoustic smearing over time. Despite this mechanistic difference, both forms of redundancy produce similar downstream consequences, namely attention dispersion and late-layer decision instability, which supports the hypothesis that information density is the critical variable. Nevertheless, the discrete manipulation does not capture all aspects of how speech encodes information, and future work should develop interventions that more faithfully emulate the continuous nature of acoustic redundancy.

The modest improvements from KV token merging, ranging from +0.1 to +0.5 percentage points as shown in Table 5, suggest that the modality gap is not merely a matter of token quantity. Even after merging, speech tokens may still carry noise, prosodic variation, and non-semantic information that text tokens do not. This points to a distinction between token redundancy and token quality. Text tokens are highly compressed symbolic units, whereas speech frames, even when merged, retain acoustic residue that may interfere with late-layer sharpening. These observations motivate more sophisticated semantic compression techniques, such as learned abstractors or hierarchical pooling, that selectively retain task-relevant content rather than simply reducing token count. We leave the design and evaluation of such methods to future work.

## I. Implementation Details

### I.1. Hyperparameters and Setup

Key implementation choices that affect all analyses are reported below. Table 7 lists the shared settings used for DTW and CKA analyses in this paper.

Parameter	Value or Method
<i>Hidden State Extraction</i>	
Extraction Window	Last user segment, i.e., question turn only
Valid Tokens	Positions where <code>attention_mask=1</code>
<i>DTW Alignment</i>	
Base Layer $\ell_0$	Layer 10 for SpeechMMLU, Layer 20 for BBH
Metric	Cosine similarity with per-row normalization
Step Penalty $\lambda$	0, i.e., standard DTW
Band Constraint	None, i.e., unconstrained
<i>Cross-Layer Aggregation</i>	
Item Selection	Fixed set of 100 items with seed 0
CKA Method	Linear CKA with double-centering

Table 7. Summary of implementation hyperparameters.